

Conceptual Design and Performance Prediction of a Thermosyphon Solar Water Heating System using TRNSYS

Z. S Johnson ^a, G.Y Pam ^b K. M Peter ^c

a. Department of Mechanical Engineering Plateau State Polytechnic Barki Ladi Jos Nigeria

b. Department of Mechanical Engineering, Ahmadu Bello University Zaria. Nigeria

c. Department of Mechanical Engineering, University of Jos. Nigeria

Abstract - This study is the design and performance simulation of a solar domestic hot water thermosyphon system for Zaria Nigeria latitude 11.2 °N and longitude 7.8°N. The design method employed is the simulation based method, where detailed mathematical models representing the design procedure of each component and whole system design is coded into a computer program using MATLAB programming language. The program was used to calculate collector design parameters and system characteristics. The effect of some collector design parameters such collector tube diameter, absorber plate thickness and collector tube center to center distance on the heat removal factor were studied through an optimization program written in Matlab programming language to determine their optimal values using . The performance of the system was simulated using TRNSYS 16 software based on the optimal design parameters to predict the storage tank and collector temperature at the end of an average recommended day for each month of the year. The final system configuration and size adopted (Table 2) based on the result of the optimisation, reveals that storage tank water temperature varies between 59 to 82 degrees Celsius at the end of each day for all year round performance for this location. This implies that a very significant fraction of the system load of a monthly average daily hot water demand of 0.1m³ set at 90°C is made by the solar water heater indicating potentials in reduction of family utility bill for heating water.

Keywords: Tank Storage Temperature; Flat-plate collectors; Solar fraction; TRNSYS

1. INTRODUCTION

The Sun emits energy at a rate of 3.8×10^{23} KW, of which, approximately 1.8×10^{14} KW is intercepted by the earth, which is located about 150 million km from the sun. About 60% of this amount reaches the surface of the earth. The rest is reflected back into space and absorbed by the atmosphere. About 0.1% of this energy, when converted at an efficiency of 10% would generate four times the world's total generating capacity of about 3000 GW [1]. It is also worth noting that the total annual solar radiation falling on the earth is more than 7500 times the world's total annual

primary energy consumption of 450 EJ [1]. The annual solar radiation reaching the earth's surface, approximately 3,400,000 EJ, is an order of magnitude greater than all the estimated (discovered and undiscovered) non-renewable energy resources, including fossil fuels and nuclear energy [1]. However, 80% of the present worldwide energy used is based on fossil fuels. Risks associated with their use are that they are all potentially vulnerable to adverse weather conditions or human acts. World demand for fossil fuels (starting with oil) is expected to exceed annual production, probably within the next two decades. International economic and political crisis and conflicts can also be initiated by shortages of oil or gas. Moreover, burning fossil fuels release harmful emissions such as carbon dioxide, nitrogen oxides, aerosols, etc. which affect the local, regional and global environment.

The heat converted from solar radiation, is well suited to provide domestic hot water and space heating. However satisfactory performance and reliability of a solar water heating system requires proper design to adequately size its components as well as accurate prediction of the delivered useful energy and outlet water temperature [2] .

There has been, extensive work on the analysis of the performance of thermosyphon solar water heaters, both experimentally and analytically, by numerous researchers: Belessiotis and Mathioulakis, [3] developed an efficient and simple simulation approach for thermosyphon solar water heaters and used the proposed methodology for energy optimization of the system in the design phase and for evaluation of test results of an existing system in order to improve it further. Shariah and Shalabi [4] have studied optimization of design parameters for a thermosyphon solar water heater for two regions in Jordan represented by two cities, namely Amman and Aqaba through the use of TRNSYS simulation program. Their results indicate that the solar fraction of the system can be improved by 10 to 25% when each studied parameter is chosen properly.

Zerrouki et al. [6] and Belessiotis and Mathioulakis [3] conducted their work on thermosiphon solar water heaters without heat exchanger. The first researchers took, as parameters of their study, the storage tank average

temperature and the water mass flow rate in the system. No allusion is, however, made to the inlet and outlet water temperatures from the collector and also the inlet and outlet temperatures of the storage tank, which are essential parameters to evaluate the energy of the system. Subsequent researchers undertook numerical and experimental studies with the aim of exploiting the results to bring a better comprehension of the basic operation of the system and also in order to optimize and improve its design.

2. SYSTEM DESCRIPTION (THERMOSYPHON):

The system consists of a flat plate solar collector, tilted from the horizontal, a thermally insulated horizontal storage tank and interconnecting pipes connecting the solar collector and the storage tank. The flat plate collector casing is made of dry wood to minimize heat loss. The flat plate collector has evenly spaced copper pipes called risers embossed by semi-circular grooves formed in the flat plate absorber. The casing is covered at the top with a 4 mm

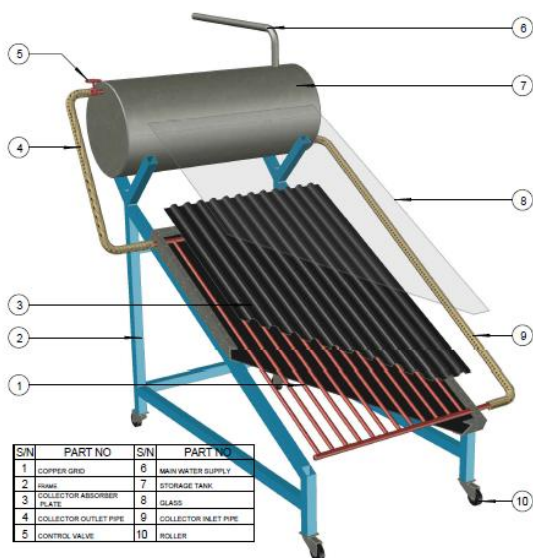


Fig. 1. Exploded view of the thermosyphon water heating system.

- 1-Copper Grid
- 2-Supporting Frame
- 3-Collector Absorber Plate.
- 4-Collector Outlet Pipe
- 5-Storage Tank Inlet Control Valve.
- 6- Mains Water Supply Pipe.
- 7-Hot Water Storage Tank
- 8- Glass Glazing
- 9- Tank Outlet Pipe
- 10- Roller.

2. System Design theory.

2.1 Flat Plate Solar Collector Design Equations

2.1.1 **Collector heat removal factor:** In designing a flat plate collector one important design parameter that need to be determined is the heat removal factor F_R . F_R is analogous to the heat exchanger effectiveness. For a header-riser flat-plate

thick glass sealed with a rubber gasket. The absorber plate is painted with black fine matte paint to achieved high absorption coefficient. The underside of the absorber insulated with dry wood to reduce conduction losses. The hot water storage tank made from PVC material is properly lagged with saw dust to minimize heat loss to the surroundings. The hot water storage tank is linked to a source of water from the mains water supply through the cold water inlet as seen in figure 1. Control valves to control the inflow of water into the storage tank from the main supply are incorporated along the length of the pipe linking the mains water supply to the storage tank. To prevent draining back of water into the collector when the temperature in the collector is lower than that in the tank, especially in the night when there is no solar radiation, another control valve is put between the pipe connecting the collector hot water outlet and storage tank hot water inlet. The hot water to meet the domestic load is collected through the hot water outlet.

collector, the collector heat removal factor is expressed as [8].

$$F_R = \frac{\dot{m} C_p}{A_c U_L} \left[1 - \exp \left(- \frac{A_c U_L F'}{\dot{m} C_p} \right) \right] \quad (1)$$

Where:

$$F' = \frac{1/U_L}{W \left[\frac{1}{U_L D_i + (W - D_i) F} + \frac{1}{c_b} + \frac{1}{\pi D_i h_{fi}} \right]} \quad (2)$$

F is the standard fin efficiency for straight fins with rectangular profile, given as:

$$F = \frac{\tanh \left[\frac{m(W - D_i)}{2} \right]}{\frac{m(W - D_i)}{2}} \quad (3)$$

$$\text{Where : } m = \sqrt{\frac{U_L}{K \delta_t}} \quad (4)$$

2.1.2 Thermal Losses in a Flat-Plate Collector

Heat losses from any solar water heating system take the three modes of heat transfer: radiation, convection and conduction. The conduction heat losses occur from sides and the back of the collector plate. The convection heat losses take place from the absorber plate to the glazing cover and can be reduced by evacuating the space between the absorber plate and the glazing cover and by optimizing the gap between them [9].

An approximate relation for collector top loss coefficient (U_{top}) given by [8] is expressed as:

$$U_{top} = \frac{1}{\frac{N_G}{C} \left[\frac{T_{pm} - T_a}{N_G + f} \right]^e + \frac{1}{h_w}} + \frac{[\sigma (T_{pm}^2 + T_a^2)] [T_a + T_{pm}]}{\frac{1}{\varepsilon_p + 0.00591 N_G h_w} + \frac{2 N_G + f - 1 + 0.133 \varepsilon_p}{\varepsilon_g} - N_G} \quad (5)$$

Where:

$$f = (1 + 0.089h_w - 0.1166h_w \varepsilon_p)(1 + 0.07866N_G) \quad (6)$$

$$C = 520[1 - 0.000051\beta^2] \quad (7)$$

$$e = 0.430 \left(1 - \frac{100}{T_{pm}}\right) \quad (8)$$

A reasonable guess for T_{pm} for liquid heating collector operated at typical flow rates of 0.01 to 0.02kg/m²s is [8].

$$T_{pm} = T_{ci} + 10 \quad (C^o) \quad (9)$$

The energy loss through the bottom of the collector is made up of conductive loss to heat flow through the insulation and convection and radiation resistance to the environment. The magnitude of the conduction and radiation loss compared to the radiation loss is such that the radiation is negligible [8]. Thus the back loss coefficient is estimated as [8].

$$U_b = \frac{K_{bi}}{x_{bi}} \quad (10)$$

The edge loss coefficient is the ratio of the thermal conductivity of the insulation at edge to its thickness; times the ratio of the area of edge to the collector effective aperture area. Tabor (1958) recommends edge insulation of about the same thickness as the bottom insulation. The edge loss estimated by assuming one-dimensional sideways heat flow around the perimeter of the collector system is expressed as: [10].

$$U_e = \frac{K_{ei} A_e}{x_{ei} A_c} \quad (11)$$

The overall heat loss coefficient for a flat plate collector is composed of the top loss coefficient, the edge loss coefficient and the back loss coefficient. A relation for collector overall heat loss coefficient U_L is expressed as [8]:

$$U_L = U_t + U_e + U_b \quad (12)$$

2.1.3 Collector useful energy: In steady state, the performance of a flat-plate solar collector can be described by the useful gain from the collector, Q_u , which is defined as the difference between the absorbed solar radiation and the thermal loss expressed as [8]:

$$Q_u = F_R [S - U_L(T_i - T_a)]^+ \quad (13)$$

The + superscript indicates that only positive values of the terms in the square brackets are to be used. Thus, to produce useful gain greater than zero the absorbed radiation must be greater than the thermal losses.

2.1.3 Convective Heat Transfer Coefficient in tubes

The general correlation for obtaining the convective heat transfer coefficient in tubes which is a useful parameter for the calculation of the heat removal factor is expressed as [11]:

$$h_f = \frac{K_f Nu_D}{D_i} \quad (14)$$

However, the Nusselt number is a function of the Reynolds number. For the evaluation of the Nusselt number Nu_D for a laminar flow where Reynolds number is less than 2200 as in the case of thermosyphon system, Fallziah et al [12] correlated Nusselt number as:

$$Nu_D = 3.7 + \left[\frac{0.0534 \left(\frac{Re Pr D_i}{L}\right)^{1.15}}{1 + 0.0335 \left(\frac{Re Pr D_i}{L}\right)^{0.82}} \right] \quad (15)$$

Where Re is the Reynolds number expressed by Incropera, et al. [13]. as:

$$Re = \frac{4\dot{m}}{\pi D_i \mu} \quad (18)$$

Pr is the Prandtl number expressed by Duffie and Beckman [8] as:

$$Pr = \frac{c_p \mu}{K_f} \quad (19)$$

2.2 System Load Calculation

In this system design, the load is calculated by summing the amount of energy needed to heat water to the desired temperature (sensible heat requirement) and any heat loss from the storage tank and piping system [14] (Annas 1998).

$$Q_s = Q_L + Q_p + Q_{st} \quad (20)$$

For satisfactory performance of the system, the collector useful energy gain should be greater than the system total load. i.e $Q_u > Q_s$

2.2.1 Sensible Heat Requirement.

The sensible heat requirement is the energy needed to raise the temperature of water to desired temperature. If water of volume V is to be heated from a mains supplied temperature T_i to a desired temperature T_L , the energy requirement over a specified time horizon may be expressed as follows [15]:

$$Q_L = \rho V C_p (T_L - T_i) \quad (21)$$

When the storage tank temperature is less than the load (desired) temperature ($T_{st} < T_L$), the desired load temperature requirement can be met by an auxiliary heater. The duty of auxiliary heater is given by the formula [15].

$$Q_{aux} = \rho V C_p [T_L - T_{st}] \quad (22)$$

2.2.2 Pipe/Ducts Losses.

These can be estimated by conventional methods. For any well-designed system the losses from ducts should be small and can be approximated to an adequate degree of accuracy in terms of the inlet and outlet temperatures as [8] :

$$Q_p = U_i A_i (T_i - T_a) + U_o A_o (T_o - T_a) \quad (23)$$

2.2.3 Storage Tank Losses.

Losses from the storage tanks may be significant. The rate of tank losses is estimated from the tank loss coefficient-area product $(UA)_{st}$ and the ambient temperature T_a surrounding the tank, as [15] :

$$\dot{Q}_{StL} = U_{st} A_{st} (T_{st} - T_a) \quad (24)$$

2.3 System Performance Evaluation

2.3.1 System Solar Fraction:

Solar fraction is the fraction of the total hot water energy need that is supplied by solar system, is calculated using the equation from Buckles and Klein [16].

$$SF = \frac{Q_L - Q_{Aux}}{Q_L} \quad (27)$$

Q_{Aux} is the total auxiliary energy supplied to the system to support the portion of the total load that is not provide by the solar energy. The solar fraction is a better indicator of the system performance compared to the other parameters such as collector efficiency or heat removal factor, since it manifests the overall performance of the entire system not a component Buckles and Klein [16] .

2.3.2 Collector Efficiency

The Hottel-Whillier equation defines the efficiency for a solar collector in terms of the collector heat removal factor F_R , given in equation form as [17]:

$$\eta_C = \frac{Q_u}{H_T A_c} = \frac{F_R [S - U_L (T_i - T_a)]^+}{H_T} \quad (28)$$

3. Design Approach and Methodology

The bulk of the design of this solar water heating system is to appropriately size the flat plate solar collector to meet the system load and remain within the operating parameters of the materials through numerical simulation.

3.1 Weather Data and the Design Month:

Solar radiation and meteorological data which are very important driving functions for all solar system design often seem to be highly random and irregular. However, long-term statistical analysis indicates that these variables are predictable to some degree. The dynamic nature of solar data can therefore be smoothed out by formulating a representative data which can characterized the mean-value behavior of any location over a long period [7]. Based on this method, the Typical Meteorological Year (TMY) weather data obtained from www.weatheranalytic.com for the location (Zaria) latitude 11.2° N and longitude 7.8° E will be processed using the type 109 TRNSYS component

to obtain monthly average daily values of: Ambient temperature, wind velocity and total radiation on tilted surface, for typical recommended day of each month of the year as shown in table 1 [7]. The month with the worst amount of total radiation on collector surface tilted at angle equal to latitude of Zaria (11.2°) is considered as the design month. System design parameters optimization and characteristics would be calculated based on the solar radiation and weather data of the design month.

3.2 Design Calculation and Optimisation Procedure

To determine the flat plate design parameters and system characteristics, required to provide 0.1m^3 of hot water set at 90°C at the end of each day, equations (1) to (28) were coded using Matlab programming language in a way that represents the design sequence calculations. Solar radiation and weather data for the design month served as input to these calculations. To optimize the collector design parameters, an optimization program written in Matlab programming language was use to study the sensitivity and effect of varying some of the selected design parameters on the objective function (the heat removal factor). The results for the optimizations are not shown in this publication. Table 2 shows the results of the design calculations and the system characteristics from the optimization results used for the performance simulation.

3.3 System Performance Prediction

The annual performance of the system was evaluated by simulating the collector and storage tank water temperatures for typical average recommended day of the months using TRNSYS 16 software based on the system characteristics and optimal design parameters as presented in table 2.

4. Results And Discussion

Table 1 shows the monthly average daily total solar radiation on tilted surface (11.2°) and weather data of Zaria, Nigeria (lat. 11.2° N and Long. 7.8° E) for recommended average day of the months obtained by processing the Typical Meteorological Year (TMY) weather data using the Type 109 solar radiation processor

of TRNSYS 16 software . The The table shows that the month of August has the worst amount of solar radiation. This month is used as the design month. The solar radiation and weather data of this month (August) served as the input for the calculations of system designs parameters and parametric study to determine the optimum system parameters for the performance simulation of the system.

Table 1: Simulated monthly average daily solar and weather data for Zaria for typical average recommended of the months .

	V (m/s^2)	T_a ($^\circ C$)	H_T ($J/m^2 \cdot day$)
JAN	2.60	38	26.8×10^6
FEB	2.57	38	27.5×10^6
MARCH	2.70	40	27.7×10^6
APRIL	2.31	32	26.8×10^6
MAY	2.80	35	26.1×10^6
JUNE	3.50	32	21.2×10^6
JULY	2.91	26	16.2×10^6
AUGUST	3.08	28	15.1×10^6
SEPT	1.56	32	24.0×10^6
OCT	2.57	36	23.7×10^6
NOV.	3.39	35	24.9×10^6
DEC.	2.00	33	26.5×10^6
A. AV	2.67	33.75	23.1×10^6

Source: Researcher simulated result

4.2 System Optimum Design Parameters and Simulation

Table 2 shows the final optimum system design parameters and components sizes obtained from the optimization procedures of the system using solar radiation and weather data of the design month (August). These system characteristics (table 2) were used to evaluate and predict the performance of the system in August and other months. Figure 1 to figure 6 shows the predicted performance of the system at the end of the day based on the TMY solar radiation and weather data for each typical recommended average day of each month of the year. From these figures, the system is capable of heating water to temperature above $75^\circ C$ from the months of January to April. This implies that the system is capable of meeting 83% of the designed load of $0.1 m^3$ of hot water set at temperature of $90^\circ C$. The figures also indicate a drop in average tank temperature at the end of the day from the months of May to August, with

the worst condition in August ($54^\circ C$). This may be due to poor weather conditions experience during these months as a result of high amount of rainfall resulting to high cloud cover reducing the amount of solar radiation received on the collector surface. The performance of the system again improved from the months of September to December due to less cloudy conditions leading to higher solar radiation as the rains is lesser in these months.

Table 2a: System components characteristics.

Description	Value/Type
Riser tubes material	Copper
Number of riser tubes	12
Absorber surface	Painted matt black
Glass type	4 mm low iron glass

Table 2b: System final optimum design parameters and components size used for the simulation.

Orientation:	Sloped towards true south	
Parameter	Description	Values
A_c	Collector area (m ²)	2.20
$F_R(\tau\alpha)_n$	Heat removal factor-transmittance-absorbance product	0.63
$F_R U_L$	Heat removal factor-collector loss coefficient product	14.26
\dot{m}	Mass flow rate per unit collector area (kg/h m ²)	16.00
b_o	Incidence angle modifier constant	0.10
β	Collector slope (degrees)	12.0
N_R	Number of parallel collector risers	12
d_R	Riser diameter (m)	0.02
H_d	Header diameter (m)	0.02
H	Header length (m)	1.4
h_c	Vertical distance between collector outlet and inlet (m)	0.33
h_o	Vertical distance between outlet of tank and inlet of collector (m)	0.37
d_i	Diameter of collector inlet pipe (m)	0.02
L_i	Length of collector inlet pipe (m)	2.0
U_i	Loss coefficient of collector inlet pipe plus insulation (kJ/h m ² °C)	0.625
d_o	Diameter of collector outlet piping (m)	0.02
L_o	Length of collector outlet piping (m)	0.80
NB_2	Number of right angle bends (or equivalent) in collector outlet piping	2
U_o	Loss coefficient of collector outlet pipe plus insulation (kJ/h m ² °C)	0.625
V_t	Tank volume (m ³)	0.120
H_t	Tank height (if vertical) or diameter (if horizontal) (m)	0.40
H_R	Height of collector return to tank above bottom of tank (m)	0.39
C_p	Fluid specific heat (kJ/kg °C)	4.19
ρ_{fs}	Fluid density at standard conditions (kg/m ³)	1000

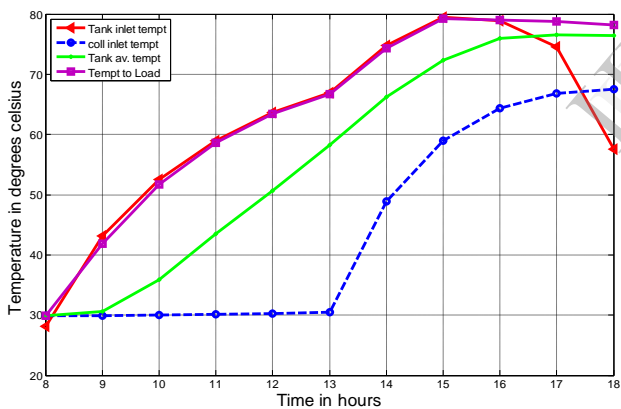


Figure 1: Temperatures variation for a recommended average day in January. (17th January)

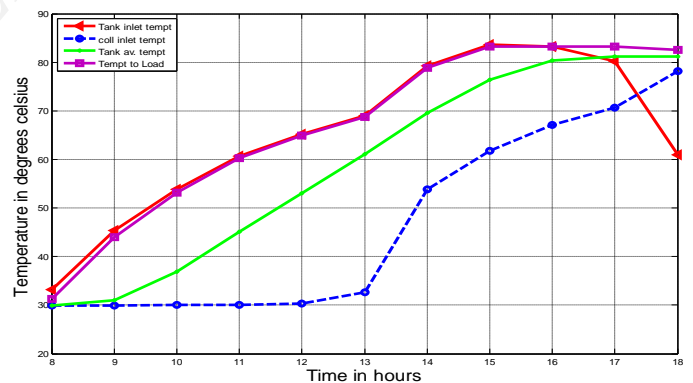


Figure 3: Temperatures variation for a recommended average day in March. (16th March)

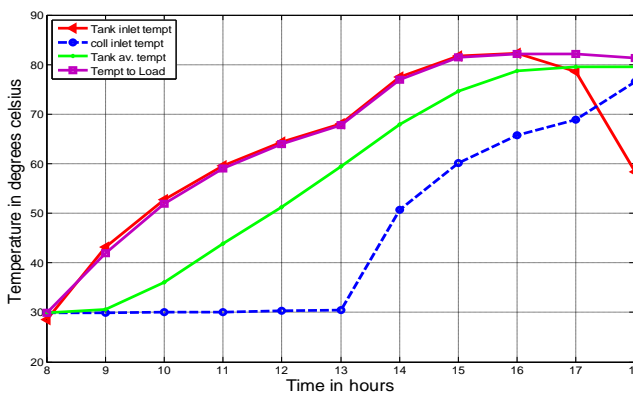


Figure 2: Temperatures variation for a recommended average day in February. (16th February)

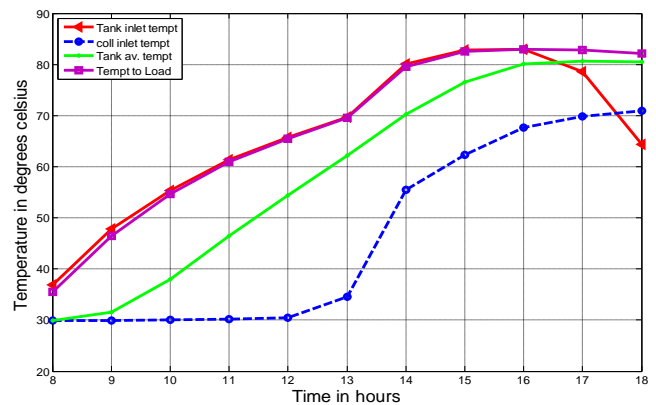


Figure 4: Temperatures variation for a recommended average day in April. (15th April)

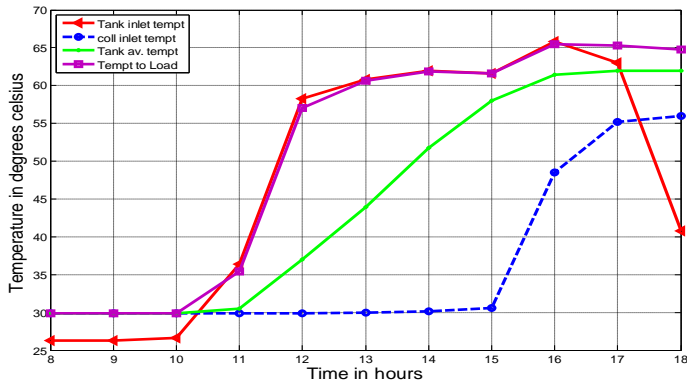


Figure 5: Temperatures variation for a recommended average day in May. (15th May)

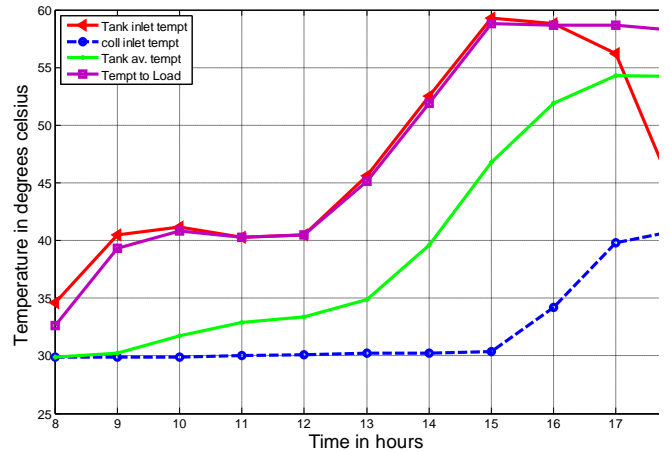


Figure.8: Temperatures variation for a recommended average day in August. (16th Aug)

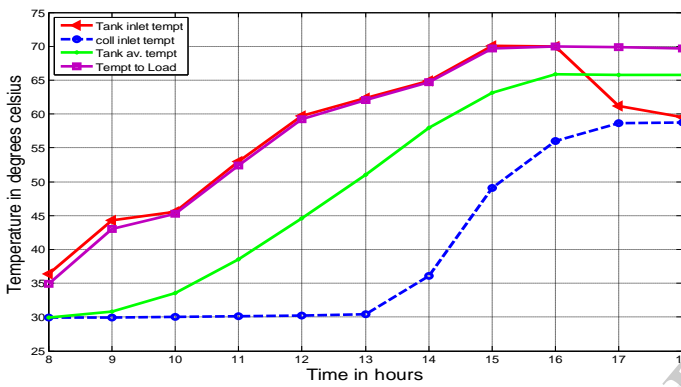


Figure 6: Temperatures variation for a recommended average day in June. (11th June)

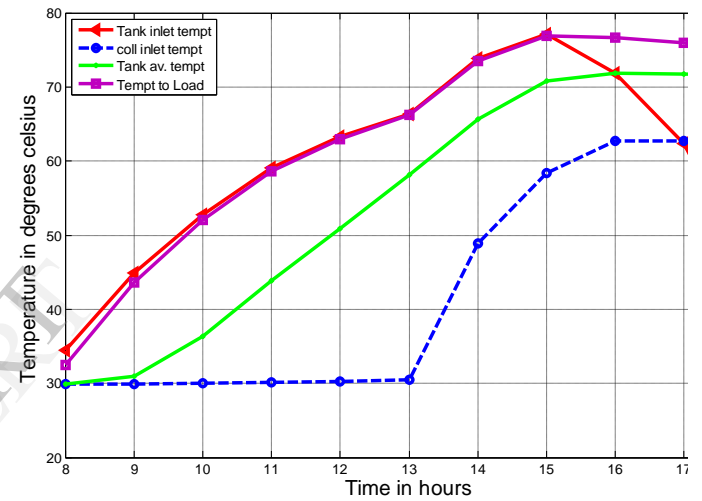


Figure 9: Temperatures variation for a recommended average day in September. (15th Sept.)

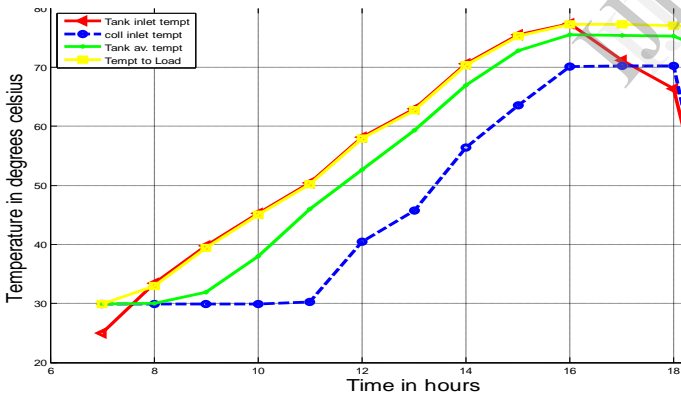


Figure 7: Temperatures variation for a recommended average day in July. (17th July)

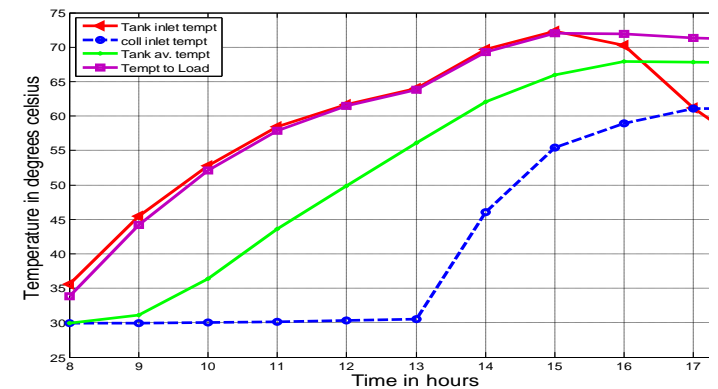


Figure 10: Temperatures variation for a recommended average day in October. (15th Oct)

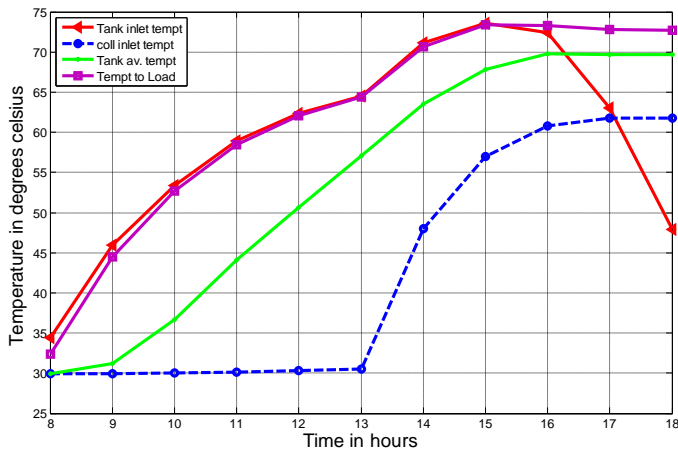


Fig.11: Temperatures variation for a recommended average day in November. (14th Nov.)

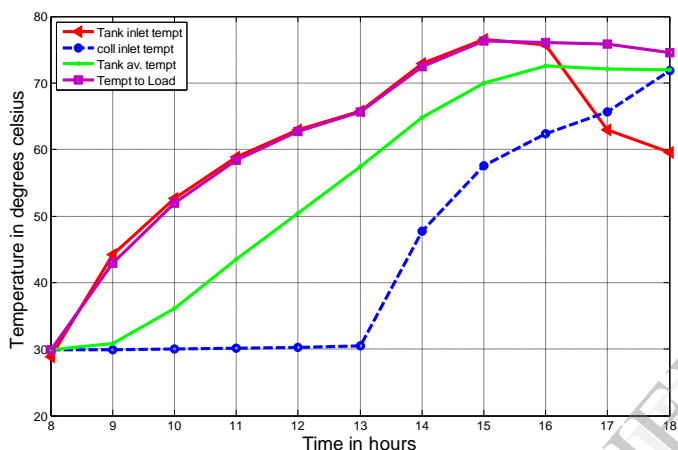


Figure12: Temperatures variation for a recommended average day in December. (10th Dec.)

5. CONCLUSIONS

A thermosyphon solar water heating system, designed to meet a daily load of 100L of hot water at 90°C was designed and the performance of the system was evaluated through simulation for Zaria using TRNSYS simulation Program. The simulated results lead to the following conclusions:

- 1 The solar system is capable of meeting 60% to 90% of the monthly average daily hot water need of 0.1m³ at 90 °C all year round with a collector area of 2.24 m²
- 2 The performance of a thermosyphon solar heating system depends on many parameters which have to be exploited through simulation and experimental studies. These studies are necessary to obtain a detailed understanding of the system behaviour which leads to more efficient designs.

REFERENCES.

- 1 Mirunalini T., Iniyar S, Ranko G. 'A review of solar thermal technologies'. *Renewable and Sustainable Energy Reviews* ,14: 312–322. (2010)
- 2 Young-Deuk K *et al.* 'Thermal analysis and performance optimization of a solar hot water plant with economic evaluation'. *Solar Energy* 86 : 1378–1395. (2012)
- 3 Belessiotis V, Mathioulakis E. 'Analytical approach of thermosyphon solar domestic hot water system performance'. *Solar Energy*; 72: 7–15. (2002)

- 4 Shariah AM, Shialabi B. 'Optimal design for a thermosyphon solar water heater'. *Renewable Energy*;11:351-361. (1997):
- 5 Kulkarni, G.N., Kedare, S.B., Bandyopadhyay, S. 'The concept of design space for sizing solar hot water systems'. *Solar Energy*: 12:283-298. (2006).
- 6 Zerrouki A, Boume'dien A, Bouhadeff K. 'The natural circulation solar water heater model with linear temperature distribution'. *Renew Energy*;26:549–559. (2002).
- 7 Qin L. 'Analysis modelling and optimum design of solar domestic hot water system'. (Phd thesis, University of Wisconsin) Retrieved 13th march 2011 at <http://sel.me.wisc.edu/theses>. (1998)
- 8 Duffie, J.A., Beckman, W.A., 'Solar Engineering of the Thermal Processes', second ed. John Wiley & Sons Inc., New York. (991).
- 9 S.N. Agbo and E.C. Okoroigwe, 'Analysis of Thermal Losses in the Flat-Plate Collector of a Thermosyphon Solar Water heater'. *Research Journal of Physics*, 1: 35-41. (2007).
- 10 Rai G.D. 'Solar energy utilization: A text book for engineering students' 5th Edition, Delhi, Khanna. (2008).
- 11 Jaime B. 'Principles and Modern applications of mass transfer operations'. New Jersey. (2009)
- 12 Fallziah, S. Balbir S. M. 'Simulation of Convective Heat Transfer Coefficient in The Receiver Tube of a Parabolic Trough Concentrator'. (2003)
- 13 Incropera, F.P., DeWitt, D.P, Bergman, T.L., & Lavine, A.S., 'Fundamentals of heat and mass transfer', 6th Ed., Hoboken, NJ, John Wiley & Sons. (2007).
- 14 Annas, H. 'Conceptual design of a solar-thermal heating system with seasonal storage for a vashon greenhouse'. (Unpublished Master's thesis, University of Washington). Retrieved Jan 20th 2012 at http://faculty.washington.edu/malte/pubs/Anna_Thesis.pdf. (2006)
- 15 Govind N. K, Shireesh B. K, Santanu B. 'Determination of design space and optimization of solar water heating systems'. *Solar Energy*;32: 263-276. (2006)
- 16 Buckles, W.E., Klein, S.A., 'Analysis of solar domestic hot water heaters'. *Solar Energy* 25 (5), 417–424. 1980.
- 17 Govind N.K., Shireesh B.K., Santanu B. 'Design of solar thermal systems utilizing pressurized hot water'. *Solar Energy*, 82 : 686–699. (2008).

NOMENCLATURE

A_c	Collector area (m ²)
A_e	Edge insulation area (m ²)
A_{st}	Tank surface area (m ²)
C_b	Contact resistance (KJ/hr.m.K).
C_p	Fluid specific heat (KJ/kgK)
D_i	Diameter of collector inlet pipe (m)
D	Outer tube diameter (m)
F_R	Heat removal factor
F'	Collector efficiency factor
F	Standard fin efficiency
h_{fi}	fluid heat transfer coefficient (KJ/hr.m ² .K).
h_w	Wind heat transfer coefficient KJ/hr.m ² .K).
H	Monthly average daily radiation on a horizontal surface (kJ./m ²)
k_f	Thermal conductivity of fluid in the tank (kJ/h m °C)
k_{ins}	Thermal conductivity of insulation material (kJ/hr m °K)
k	Plate conductivity (kJ/hr m °K)
K_{ei}	Thermal conductivity of edge insulation materials (kJ/hr m °K)
K_{bi}	Thermal conductivity of back insulation materials (kJ/hr m °K)
L	Length of each pipe (m)
N_g	Number of glass covers
\dot{m}	Collector fluid mass flow rate (kg/hr.m ²)

Q_L	Heat required to meet load (kJ/hr)
Q_{aux}	Auxiliary heat to meet load (kJ/hr)
Q_{LS}	Load met by solar energy (kJ/hr)
Re	Reynolds number
S	Monthly absorbed radiation (kJ/m ²)
T_{pm}	Mean plate temperature (K)
T_{ci}	Collector fluid inlet temperature (K)
T_a	Ambient temperatures (K)
T_{co}	Collector fluid outlet temperature (K)
T_L	Desired load (hot water) temperature, °C
t_{ins}	Thickness of insulation material (m)
T_{st}	Storage temperature (°c)
T_{fm}	Collector means fluid temperature (k)
T_{sti}	Storage tank inlet temperature (°c)
U_e	Loss coefficient edge of collector per unit aperture area (kJ/hr-m ² -K)
U_o	Loss coefficient of collector outlet pipe plus insulation (kJ/hr m ² °K)
V_t	Tank volume (m ³)
U_L	Overall Loss Coefficient (kJ/ m ² hr.k)
U_t	Collector top loss coefficient (KJ/hr.m ² .K).
U_b	Back loss coefficient (KJ/hr.m ² .K).
U_{st}	Tank loss coefficient (KJ/hr.m ² .K).
W	Tube spacing (m)
x_{ei}	Insulation thickness at the edge (m)

Greek Symbols

ε_p	Absorber plate emittance
α_p	Absorptance of absorber plate
β	Collector slope (degrees)
ϕ	Latitude of the location (Degrees)
δ_t	Absorber plate thickness (m)
ε_g	Emittance of glass (0.88)
ε_p	Emittance of plate
μ	Dynamic viscosity, (kg/m s)
ρ	Density of water (kg/m ³)
β'	Thermal cubic expansion coefficient
η_c	Collector efficiency

IJERT